



OPEN

Pre-existing adaptive immunity to the RNA-editing enzyme Cas13d in humans

Xin-Zi Emily Tang^{ID 1,2}, Shu Xuan Tan¹, Shawn Hoon² and Gene W. Yeo^{ID 1,3,4,5}✉

RNA-guided RNA-targeting nucleases, such as CRISPR-Cas13 proteins, have therapeutic potential for gene editing. Among Cas13d enzymes, Cas13d from the bacteria *Ruminococcus flavefaciens* (RfxCas13d) is of particular interest owing to its small size and high specificity. However, the existence of pre-existing immunity against RfxCas13d is unclear. In this study, we evaluated antibody and T cell responses to RfxCas13d in healthy donors using ELISA and T cell culture assays. We found RfxCas13d-reactive antibodies and CD4 and CD8 T cell responses in most donors, comparable to responses against Cas9 proteins from *Staphylococcus aureus* (SaCas9) and *Streptococcus pyogenes* (SpCas9). RfxCas13d-responding T cells could produce the inflammatory cytokines IFN-γ, TNF-α and IL-17. These findings should be taken into consideration in the development of RfxCas13d for therapy.

The discovery of CRISPR-Cas DNA-editing technologies has kickstarted the development of a plethora of therapeutics, adopting strategies such as eliminating disease-causing gene expression, repairing mutated genes, or adding new genes with new functions¹. Many of these therapeutics use the most well-studied Cas9 enzymes from *S. pyogenes* (SpCas9) and *S. aureus* (SaCas9). However, several high-profile studies have reported widespread pre-existing antibody and T cell immune responses directed against these Cas enzymes in the general population²⁻⁴, likely due to previous exposure to the source bacteria. As such, these therapeutic strategies typically aim for transient expression of Cas enzymes to reduce the likelihood of immune-mediated toxicity that may compromise their therapeutic effects.

The use of RNA-editing technologies is also rapidly growing and may provide complementary capabilities. RNA-editing enzymes do not carry the risk of permanent, off-target changes in the genome and are ideal for situations in which homology-directed repair of DNA is not feasible, such as in terminally differentiated cells such as neurons and muscle cells. RNA editing could also provide tunable systems for modulating gene expression without complete elimination. Additionally, targeted messenger-RNA edits could be used to restore functions of large genes that cannot be easily replaced by gene therapy, or to modify alternative splicing, such as in spinal muscular atrophy⁵.

Cas13 enzymes are type VI CRISPR enzymes that are RNA-guided RNA-targeting nucleases. Several groups have demonstrated the use of Cas13 enzymes, either alone or in conjunction with other enzymes, to improve and restore functions in models of frontotemporal dementia⁶, spinal muscular atrophy⁵ and X-linked nephrogenic diabetes insipidus⁷. Unlike Cas9 enzymes, Cas13 enzymes are not limited by a protospacer flanking sequence, allowing many sites

to be targetable. Their small gene and protein size enables easier packaging using adeno-associated viruses (AAVs) or lipid-based vectors, and they are thus highly suitable for therapeutic delivery. Among known Cas13 enzymes, RfxCas13d has been found to have the most robust knockdown efficiency while retaining high specificity and minimal off-target effects in mammalian cells^{6,8}. RfxCas13d has also been successfully delivered in vivo to modulate cholesterol metabolism and improve Parkinson's disease in mouse models^{9,10}. Because RfxCas13d could be a promising therapeutic candidate, we asked whether the general population has pre-existing immunity directed against RfxCas13d, similar to SpCas9 or SaCas9.

Here, we were able to detect antibody responses to RfxCas13d, at a level comparable with responses to SaCas9 and SpCas9. We also detected CD4 and CD8 T cell proliferative responses and characterized the cytokine profile of T cells responding to RfxCas13d. The inflammatory responses directed against RfxCas13d are an important consideration in therapeutic use of RfxCas13d.

To test whether human populations may have pre-existing humoral responses to RfxCas13d, we developed an ELISA assay to detect immunoglobulin G (IgG) antibodies in human plasma. For comparison, we expressed and purified recombinant SpCas9 and SaCas9 by the same procedures as those we used for RfxCas13d. We also used the same method to express and purify recombinant green fluorescent protein (GFP) as a negative control to detect other co-purified substances that may bind human IgG non-specifically. Of the 22 samples tested, 3 had higher background IgG binding to GFP than to the Cas proteins, and these were excluded from the analysis. For the remaining samples, the distribution of concentrations of IgG that bound RfxCas13d was comparable to the concentrations of IgG that bound SpCas9 and SaCas9, and was significantly higher than the concentrations of IgG that bound GFP (Fig. 1a). For RfxCas13d, 17/19 (89%) samples had IgG readings above the GFP background. For both SpCas9 and SaCas9, 18/19 (95%) samples had IgG readings above the GFP background (Extended Data Fig. 1a). In comparing antibody responses between Cas proteins, 13/19 samples had higher IgG readings for RfxCas13d than for SpCas9, and 8/19 samples had higher IgG readings for RfxCas13d than for SaCas9 (Extended Data Fig. 1b).

Our ability to detect antibody responses to RfxCas13d suggests that RfxCas13d-specific T cells are present because CD4 T cell help is necessary for production of high-affinity antibodies and IgG antibody class switching. To test for pre-existing T cell immunity against RfxCas13d, peripheral blood mononuclear cells (PBMCs) were cultured in the presence of recombinant RfxCas13d, and antigen-induced proliferation was measured. As a comparison, PBMCs were also stimulated with SpCas9 and SaCas9. Recombinant

¹Department of Physiology, Yong Loo Lin School of Medicine, National University of Singapore, Singapore, Singapore. ²Molecular Engineering Laboratory, Institute of Molecular and Cell Biology, Agency for Science, Technology and Research, Singapore, Singapore. ³Department of Cellular and Molecular Medicine, University of California, San Diego, La Jolla, CA, USA. ⁴Stem Cell Program, University of California, San Diego, La Jolla, CA, USA. ⁵Institute for Genomic Medicine, University of California, San Diego, La Jolla, CA, USA. ✉e-mail: geneyeo@ucsd.edu

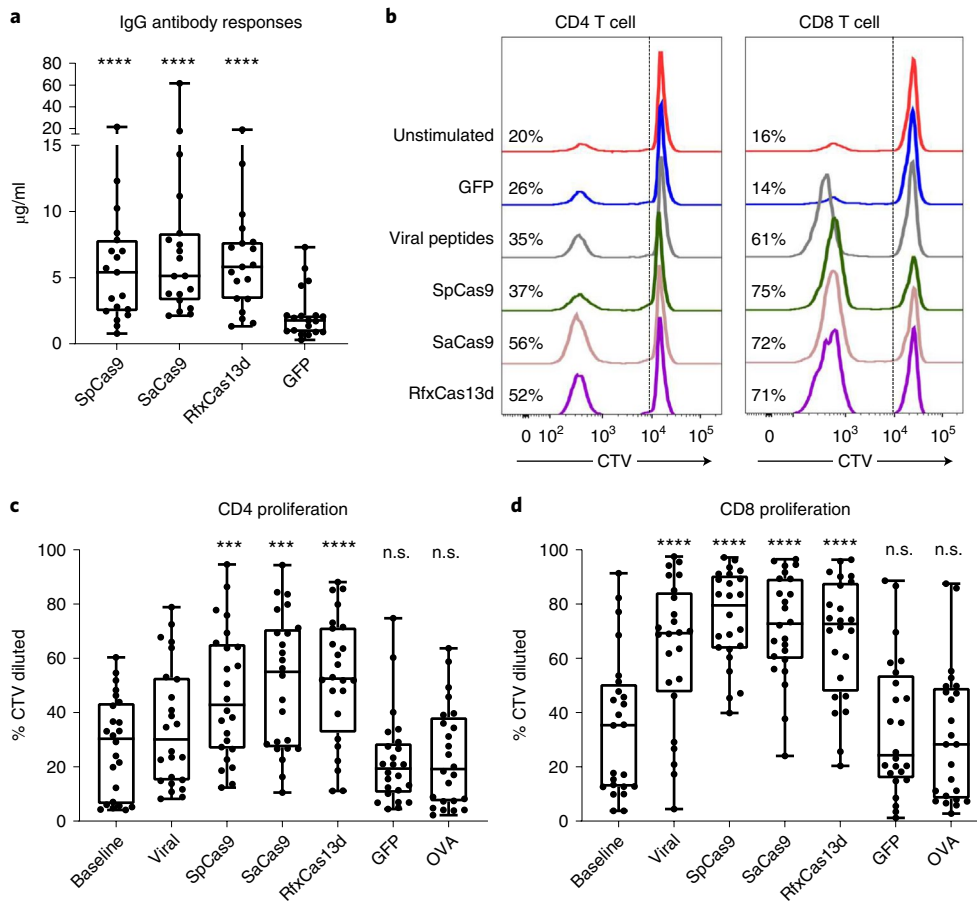


Fig. 1 | Antibody and T cell responses to RfxCas13d. **a**, IgG antibody responses to Cas proteins and GFP detected in human plasma in a direct ELISA assay ($n=19$ biologically independent samples). **b**, Representative flow cytometric analyses of CD4 and CD8 T cell proliferation following stimulation with Cas proteins. Percentages indicate the frequency of proliferated cells within the CD4 or CD8 T cell subset. **c,d**, Aggregate data showing the frequency of proliferated CD4 (**c**) or CD8 (**d**) T cells ($n=24$ biologically independent samples). Baseline indicates PBMCs cultured without antigen stimulation. Viral indicates stimulation with a pool of viral peptides. OVA, ovalbumin. Each data point represents one sample. Each sample was tested across all conditions shown in each graph. * $P < 0.05$; ** $P < 0.01$; *** $P < 0.001$; **** $P < 0.0001$; n.s., not significant. One-way ANOVA with Dunnett's multiple comparisons test on log transformed data using GFP as control (A). One-way analysis of variance (ANOVA) with Dunnett's multiple comparisons test using baseline as control (**c,d**). For box plots, the center line indicates the median, box limits indicate the 25th and 75th percentiles, whiskers show minimum to maximum values and all individual data points are shown.

GFP similarly purified and certified endotoxin-free ovalbumin were used as negative controls. A pool of viral peptides from cytomegalovirus, Epstein–Barr virus, influenza and tetanus was used as a positive control for the assay. GFP- and ovalbumin-induced proliferation was comparable with that in unstimulated samples, demonstrating that our protein preparation did not contain other immunostimulatory substances. Antigen-induced proliferation was significantly higher than in unstimulated cultures for all 3 Cas proteins tested (Fig. 1b–d). We were able to detect antigen-induced proliferative responses in the CD8 T cell compartment in 23/24 (96%) samples for RfxCas13d, SpCas9 or SaCas9. For the CD4 T cell compartment, we detected antigen-induced proliferative responses in 22/24 (92%), 21/24 (88%) and 24/24 (100%) samples after exposure to SpCas9, SaCas9 or RfxCas13d, respectively. These data indicate that most individuals have existing immune recognition of RfxCas13d, comparable with that of SpCas9 and SaCas9.

To further probe the cytokine potential of responding T cells, we restimulated expanded cells with autologous antigen-presenting cells (APCs) and recombinant Cas proteins on the final day of culture. Our gating strategy analyzes CD4 and CD8 T cell compartments separately, focusing on cytokine production in proliferated

T cells to identify antigen-responding cells that were expanded in culture (Extended Data Fig. 2). In the CD4 T cell compartment, we observed increased IFN- γ , IL-17 and TNF- α responses to RfxCas13d, above that which was induced by GFP control (Fig. 2a,b and Extended Data Fig. 3). The cytokine responses were comparable with that induced by SpCas9 and SaCas9. We were not able to detect any T cells producing IL-10 (Extended Data Fig. 3). Further analysis of samples in which both antibody and T cell data were available (13 samples, 3 Cas proteins, 39 paired readings) found that antibody responses and T cell responses are not correlated (Extended Data Fig. 4). Overall, we noted antigen-induced inflammatory cytokine production of IFN- γ or IL-17 by the CD4 T cells in 15/24 (62%, SpCas9), 20/24 (83%, SaCas9) and 21/24 (88%, RfxCas13d) samples.

In the CD8 T cell compartment, we did not observe significant IFN- γ or TNF- α cytokine production higher than that induced by GFP stimulation at the population level (Extended Data Fig. 5), although we did observe IFN- γ or TNF- α cytokine levels above background in a handful of tested individuals. The whole recombinant proteins we used for restimulation are likely to be captured by the exogenous pathway for antigen presentation, to be presented predominantly on major histocompatibility complex (MHC) class

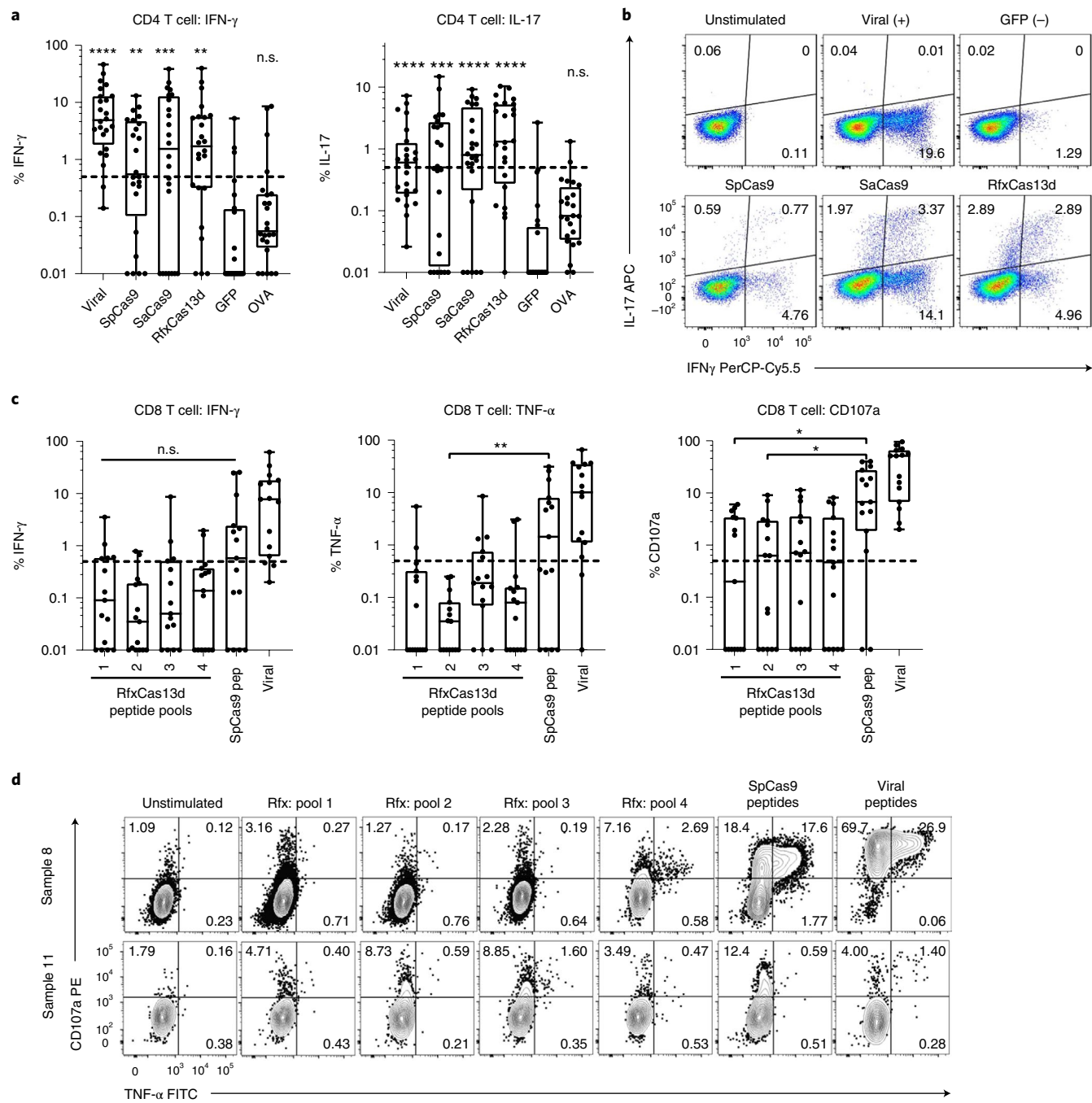


Fig. 2 | Cytokine profile of RfxCas13d-specific T cells. **a,b**, CD4 T cell responses following Cas protein restimulation on the last day of culture. **c,d**, CD8 T cell responses following overlapping peptide restimulation on the last day of culture. **a,c**, Aggregate responses are shown, with each data point representing one sample. (**a**, $n=23$ biologically independent samples. **c**, $n=15$ biologically independent samples.). Each sample was tested across all conditions shown. To ensure cytokine responses are indeed from cells expanded by antigen stimulation, each data point plots values after subtracting background responses from controls expanded with no antigen but re-stimulated with the tested antigen. Viral indicates stimulation with a pool of viral peptides. Differences in treatment conditions were tested using Friedman's test with two-sided Dunn's multiple comparisons test using GFP as the control (**a**) or across the SpCas9 and 4 RfxCas13d peptide pools (**c**). * $P < 0.05$; ** $P < 0.01$; *** $P < 0.001$; **** $P < 0.0001$. For box plots, the center line indicates the median, box limits indicate the 25th and 75th percentiles and whiskers show minimum to maximum values. The dashed line indicates the limit of detection for antigen-specific responses. **b**, Representative flow cytometric analysis of CD4 T cell cytokine responses from one sample is shown. **d**, Flow cytometric analysis of CD8 T cell cytokine responses from two samples. Sample 8 shows TNF- α responses above background to RfxCas13d peptide pool 4, SpCas9 peptides and viral peptides. Sample 11 shows TNF- α responses above background to RfxCas13d peptide pool 3 and viral peptides.

II rather than MHC class I molecules, potentially leading to an underestimation of CD8 T cell responses. We proceeded to evaluate CD8 T cell responses using overlapping 15-mer peptides spanning

the whole RfxCas13d protein, pooling the peptides into 4 pools. In parallel, we also stimulated PBMCs with overlapping 15-mer peptides spanning SpCas9 protein, for which others have demonstrated

pre-existing CD8 T cell responses^{3,11}. Our assay provided minimal stimulation for short-term expansion of memory T cells with low chance of a false positive, as demonstrated by responses below background for both GFP and ovalbumin; therefore, no negative control peptides were used. CD8 T cell responses directed against peptides from RfxCas13d were detectable, but were of considerably lower magnitude than responses directed against peptides from SpCas9. We identified IFN- γ or TNF- α cytokine responses to at least one of the four peptide pools in 11/15 (73%) samples and CD107a upregulation in 12/15 (80%) samples, indicating cytotoxic capacity (Fig. 2c,d). For SpCas9 CD8 T cell responses, 9/15 (60%) samples showed IFN- γ or TNF- α cytokine responses, and 13/15 (87%) samples showed CD107a cytotoxic responses. We also observed CD4 T cell production of IFN- γ , TNF- α and IL-17 after overlapping peptide stimulation (Extended Data Fig. 6), with all samples showing cytokine responses to at least one of the four peptide pools, confirming earlier observations from protein stimulation (Fig. 2a,b).

The detection of immune responses to RfxCas13d is contrary to expectations because *Ruminococcus flavefaciens* strain XPD3002, the bacterial origin of RfxCas13d, was originally isolated from the bovine rumen and does not colonize humans. A protein BLAST search found that the next closest protein matches were Cas13d from other bacteria belonging to *Ruminococcus* sp., such as *R. bicirculans*, a dominant human colonic bacteria¹². These Cas13d proteins from related species in the human gut share 35–37% protein sequence identity (Extended Data Fig. 7), suggesting that T cells and antibodies that recognize regions with greater homology may be sufficiently cross-reactive to respond to RfxCas13d. To address this possibility, during peptide pooling for our peptide stimulation assay, we combined the peptides showing greater homology with human isolates in pool 4 and assigned the other peptides to pools 1–3. IFN- γ and TNF- α production by CD4 T cells was elevated in pool 4 (Extended Data Fig. 6), which also induced the highest CD4 IFN- γ responses among the 4 peptide pools in 8/15 samples, supporting the hypothesis of cross-reactive T cells. However, other peptide pools also induced specific responses, for example pool 1 appeared to be more effective at inducing IL-17 CD4 T cell responses (Extended Data Fig. 6) and pool 3 seemed to induce stronger TNF- α CD8 T cell responses (Fig. 2c). Immune responses against other Cas13 enzymes were not assessed in this study, so the generalizability of the findings is not yet clear. Detectable T cell responses elicited by peptide pools 1–3 suggest that amino acid sequences that do not have extensive homology to proteins derived from known bacteria strains that colonize humans may nonetheless elicit immune responses. Such responses can be identified only by empirical testing. Similarly, newly discovered Cas proteins derived from any source will have to be individually tested to determine whether they may be susceptible to immune recognition.

Our findings argue for caution in the use of RfxCas13d as a therapeutic, particularly if the enzyme is to be expressed in the long term. Because RfxCas13d will exert its effects on RNA in the intracellular space rather than in the extracellular space, we expect RfxCas13d to be more susceptible to T cell-mediated recognition and clearance than antibody recognition. Although most non-immune cells do not present peptides on MHC-II and may thus escape recognition by the RfxCas13d-reactive CD4 T cells, many organs and tissues contain tissue-resident macrophages that express MHC-II¹³, and may contribute to antigen presentation¹⁴. Our data also suggest the presence of cytotoxic CD8 T cells that recognize RfxCas13d and may play a role in eliminating cells expressing RfxCas13d.

Some have suggested the use of RfxCas13d as an anti-viral agent¹⁵ or to help eliminate cancerous cells in bladder cancer¹⁶. The immune response directed against RfxCas13d may provide an added effect in eliminating virus-infected or cancerous cells. However, IL-17-producing CD4 T cells are not the most effective T cells for killing infected or cancerous cells and may instead create

a pro-inflammatory environment leading to tissue damage. In addition, precise delivery of RfxCas13d to target cells will be required so that healthy cells expressing RfxCas13d will not be vulnerable to immune-mediated toxicity.

To avoid inflammatory immune-mediated toxicity, other gene therapy strategies have adopted immunosuppressive regimens with varying degrees of success¹⁷. Alternatively, repeated dosing using orthologues with non-overlapping immune recognition sites may allow sustained genetic edits¹⁸. It may also be possible to identify immunodominant T cell epitopes and modify them to reduce immunogenicity or MHC binding affinity^{11,19}, a strategy that has been used to deimmunize recombinant monoclonal antibodies facing issues of immune-mediated elimination. RfxCas13d may also be able to avoid immune detection if its therapeutic use is limited to immuno-privileged sites. Further studies will be required to determine whether these strategies may be sufficient to allow long-term expression and sustained genetic editing by RNA-directed RNA nucleases, such as RfxCas13d.

Online content

Any methods, additional references, Nature Research reporting summaries, source data, extended data, supplementary information, acknowledgements, peer review information; details of author contributions and competing interests; and statements of data and code availability are available at <https://doi.org/10.1038/s41591-022-01848-6>.

Received: 19 August 2021; Accepted: 28 April 2022;

Published online: 06 June 2022

References

- Tay, L. S., Palmer, N., Panwala, R., Chew, W. L. & Mali, P. Translating CRISPR-Cas therapeutics: approaches and challenges. *CRISPR J.* **3**, 253–275 (2020).
- Charlesworth, C. T. et al. Identification of preexisting adaptive immunity to Cas9 proteins in humans. *Nat. Med.* **25**, 249–254 (2019).
- Wagner, D. L. et al. High prevalence of *Streptococcus pyogenes* Cas9-reactive T cells within the adult human population. *Nat. Med.* **25**, 242–248 (2019).
- Simhadri, V. L. et al. Prevalence of pre-existing antibodies to CRISPR-associated nuclease Cas9 in the USA population. *Mol. Ther. Methods Clin. Dev.* **10**, 105–112 (2018).
- Du, M., Jillette, N., Zhu, J. J., Li, S. & Cheng, A. W. CRISPR artificial splicing factors. *Nat. Commun.* **11**, 2973 (2020).
- Konermann, S. et al. Transcriptome engineering with RNA-targeting type VI-D CRISPR effectors. *Cell* **173**, 665–676 e614 (2018).
- Cox, D. B. T. et al. RNA editing with CRISPR-Cas13. *Science* **358**, 1019–1027 (2017).
- Wessels, H. H. et al. Massively parallel Cas13 screens reveal principles for guide RNA design. *Nat. Biotechnol.* **38**, 722–727 (2020).
- He, B. et al. Modulation of metabolic functions through Cas13d-mediated gene knockout in liver. *Protein Cell* **11**, 518–524 (2020).
- Zhou, H. et al. Glia-to-neuron conversion by CRISPR-CasRx alleviates symptoms of neurological disease in mice. *Cell* **181**, 590–603 (2020).
- Ferdosi, S. R. et al. Multifunctional CRISPR-Cas9 with engineered immunosilenced human T cell epitopes. *Nat. Commun.* **10**, 1842 (2019).
- Walker, A. W. et al. Dominant and diet-responsive groups of bacteria within the human colonic microbiota. *ISME J.* **5**, 220–230 (2011).
- Gautier, E. L. et al. Gene-expression profiles and transcriptional regulatory pathways that underlie the identity and diversity of mouse tissue macrophages. *Nat. Immunol.* **13**, 1118–1128 (2012).
- Tang, X.-Z., Kreuk, L. S. M., Cho, C., Metzger, R. J. & Allen, C. D. C. Bronchus-associated macrophages are positioned for soluble antigen capture from the airway lumen and for local T_H2 cell activation. Preprint at bioRxiv <https://doi.org/10.1101/2020.09.18.247742> (2020).
- Abbott, T. R. et al. Development of CRISPR as an antiviral strategy to combat SARS-CoV-2 and influenza. *Cell* **181**, 865–876 e812 (2020).
- Zhuang, C. et al. Engineered CRISPR/Cas13d sensing hTERT selectively inhibits the progression of bladder cancer in vitro. *Front Mol. Biosci.* **8**, 646412 (2021).
- Arruda, V. R., Favaro, P. & Finn, J. D. Strategies to modulate immune responses: a new frontier for gene therapy. *Mol. Ther.* **17**, 1492–1503 (2009).
- Moreno, A. M. et al. Immune-orthogonal orthologues of AAV capsids and of Cas9 circumvent the immune response to the administration of gene therapy. *Nat. Biomed. Eng.* **3**, 806–816 (2019).

19. Jones, T. D., Crompton, L. J., Carr, F. J. & Baker, M. P. Deimmunization of monoclonal antibodies. *Methods Mol. Biol.* **525**, 405–423, xiv (2009).

Publisher's note Springer Nature remains neutral with regard to jurisdictional claims in published maps and institutional affiliations.



Open Access This article is licensed under a Creative Commons Attribution 4.0 International License, which permits use, sharing, adaptation, distribution and reproduction in any medium or format, as long as

you give appropriate credit to the original author(s) and the source, provide a link to the Creative Commons license, and indicate if changes were made. The images or other third party material in this article are included in the article's Creative Commons license, unless indicated otherwise in a credit line to the material. If material is not included in the article's Creative Commons license and your intended use is not permitted by statutory regulation or exceeds the permitted use, you will need to obtain permission directly from the copyright holder. To view a copy of this license, visit <http://creativecommons.org/licenses/by/4.0/>.
© The Author(s) 2022

Methods

Human samples. Study protocols were approved by the Institutional Review Board at the National University of Singapore (H-18-072) and at Agency for Science, Technology and Research (2018-005). PBMCs and plasma were obtained from cone blood of healthy donors with informed consent at the Health Services Authority, Singapore (201906-03). Whole blood was centrifuged at 1,600g for 10 min at room temperature, and the clear plasma layer was extracted. The plasma layer was centrifuged at 16,000g for 10 min to obtain cell-free plasma supernatant. After removing the plasma layer, the cellular fraction was diluted with sterile PBS (1st BASE) and layered on top of Ficoll (Ficoll-Paque, GE Healthcare), with 25 ml of diluted blood over 15 ml of Ficoll. The sample was centrifuged at 1,900g for 30 min at room temperature with reduced acceleration and low brakes. The PBMC layer was collected at the Ficoll-PBS interphase using a sterile Pasteur pipette and washed extensively with PBS. PBMCs were cryopreserved in CryoStor CS10 freezing medium (Stemcell Technologies) or freezing medium containing 90% FBS (Hyclone) and 10% DMSO (Hybri-Max D2650, Sigma).

Recombinant Cas proteins. For recombinant Cas protein or GFP expression, bacteria-optimized cas protein genes were synthesized (IDT) and cloned into a pET28 backbone with N-terminal 6×His-maltose-binding protein (MBP)-TEV protease cleavage site for expression from T7 promoter. His-MBP-Cas expression plasmids were sent for protein production by the Protein Production Platform (PPP) at Nanyang Technological University School of Biological Sciences (www.proteins.sbs.ntu.edu.sg). GFP was previously cloned by PPP into the pNIC28-Bsa4 backbone encoding an amino-terminal 6×His-TEV protease site. Plasmids were transformed into *Escherichia coli* BL21(DE3) Rosetta, and expression cultures were grown at 37°C using the LEX Bioreactor (Harbinger Biotech) in Terrific Broth medium supplemented with appropriate antibiotics. Upon reaching an OD₆₀₀ of 2.0, expression cultures were cooled down to 18°C before overexpression was induced by adding 0.5 mM IPTG. Cell pellets were collected at 20 hours after induction, resuspended in lysis buffer (100 mM HEPES, 500 mM NaCl, 10 mM imidazole, 10% glycerol, 0.5 mM TCEP, pH 8.0, 0.1% Nacalai Tesque protease inhibitor cocktail) and sonicated. After clarification by centrifugation at 47,000g, lysate supernatants were filtered and loaded onto an AKTAxpress system (GE Healthcare) for ion-metal affinity chromatography, followed by size-exclusion chromatography. All Ni-NTA columns (Qiagen) were washed with buffers containing 10 mM and 25 mM imidazole before proteins were eluted with elution buffer (20 mM HEPES, 500 mM NaCl, 500 mM Imidazole, 10% (vol/vol) glycerol, 0.5 mM TCEP, pH 7.5). The proteins were then subjected to size-exclusion chromatography in gel filtration buffer (20 mM HEPES, 300 mM NaCl, 10% (vol/vol) glycerol, 0.5 mM TCEP, pH 7.5) on a HiLoad 16/60 Superdex 75 prep grade column (for GFP) or Superdex 200 (for MBP-Cas). Fractions containing pure protein were pooled, supplemented with TCEP up to 2.0 mM and concentrated using Vivaspin 20 concentrators (Cytiva) before being subjected to overnight TEV protease treatment at 4°C. Samples were then loaded onto Ni-NTA columns again so we could collect the untagged proteins. Protein purity was determined to be >90% by SDS-PAGE (Supplementary Fig. 1). Endotoxins were removed using High Capacity Endotoxin Removal spin columns (Pierce, Thermo Fisher) and quantified using LAL Chromogenic Endotoxin Quantitation Kit (Pierce, Thermo Fisher). All protein preparations had less than 0.2 EU/ml of endotoxins when tested at a final concentration of 10 µg/ml. Residual *E. coli* host cell proteins were present at less than 2% in all protein preparations when tested using an *E. coli* host cell protein ELISA kit (Abcam).

ELISA. A direct ELISA assay was developed to detect IgG antibodies specific to Cas proteins. Ninety-six-well Nunc Maxisorp plates (Thermo Fisher) were coated with Cas proteins or GFP at 2 µg/ml in 100 µl of PBS (1stBASE) for 2–3 h at 37°C. For standards, wells were coated with twofold serial dilutions of purified human IgG (I4506, Sigma-Aldrich) from 320 ng/ml to 5 ng/ml. The wells were washed with Wash Buffer (PBS, 0.05% Tween 20 (Vivantis Technologies)) and blocked with 250 µl Blocking Buffer (PBS, 0.1% Tween 20 and 1% Bovine Serum Albumin (BSA, Fraction V, Gold Biotechnology)) overnight at 4°C. After 2 washes with Wash buffer, diluted plasma samples were added to the wells and incubated at room temperature for 2 hours. Plasma samples were diluted with Assay Buffer (PBS, 0.05% Tween 20 and 0.5% BSA) and tested at final concentrations of 1:20, 1:40, 1:80 and 1:160 dilutions. Readings within the linear range of standards were used to calculate IgG concentration. After extensive washing, monoclonal mouse anti-human IgG HRP (Invitrogen, Life Technologies) was used to detect bound antigen-specific IgG. After unbound antibodies were washed off, TMB Substrate solution (eBioscience, Life Technologies) was added to wells for 20 min at room temperature and Stop Solution (Invitrogen, Life Technologies) was added to halt the reaction. Absorbance was measured at 450 nm with wavelength subtraction at 570 nm on the microplate reader (Synergy HTX, Biotek Instruments) using Gen5 software (Biotek Instruments).

T cell cultures. PBMCs were rapidly thawed at 37°C and washed with a tenfold volume of RPMI (Hyclone) or DMEM (Hyclone). To measure proliferation in 10-day cultures, cells were uniformly labeled with CellTrace Violet (CTV, Life Technologies) as described²⁰. Briefly, PBMCs were resuspended in PBS (1st BASE)

with 2% AB serum (H6914, Sigma-Aldrich) and mixed in a 1:1 ratio with diluted CTV at a final concentration of 5 µM. PBMCs were incubated in a 37°C water bath for 20 minutes, with gentle mixing every 5–10 minutes. PBMCs were washed extensively and resuspended in AIM-V medium (Gibco, Thermo Fisher) with 2% AB serum. Then, 2–3 × 10⁵ cells were plated per well in a 96-well round-bottom plate (Corning) in the presence of 20 IU/ml of recombinant human IL-2 (Stemcell Technologies), as has been described²¹. PBMCs were left either unstimulated with no additional antigen or were stimulated with 5 µg/ml of recombinant Cas proteins or GFP. As an additional negative control for comparison with GFP, cells were also cultured with low-endotoxin ovalbumin (LS003061, Worthington). As a positive control, PBMCs were stimulated with 1 µg/ml of a mix of viral peptides comprising CEF peptides (Mabtech and Proimmune) to activate CD8 T cells and CEFT peptides (Proimmune) to activate CD4 T cells. For cultures stimulated with peptides, 15-mer peptides overlapping by 10 amino acids spanning the whole RfxCas13d protein was custom ordered from Genscript and pooled. Each peptide is assigned to one of four pools. The peptides present in each pool are indicated in Supplementary Table 1. Overlapping peptides for SpCas9 Pepmix was from JPT Peptide Technologies. PBMCs were stimulated with 2.5 µg/ml of each peptide with the final concentration of DMSO at less than 0.5%. For peptide-stimulated cultures, corresponding negative control wells were stimulated with 0.5% DMSO. Negative control peptides were not used with peptide-stimulated cultures because the short-term T cell expansion protocol uses minimal stimulants with low dose IL-2, synthetic peptides and no additional cytokines, co-stimulatory signals or antigen-presenting cells, thus preferentially favoring the proliferation of antigen-experienced cells over any naive cells. Recent studies using similar T cell expansion assays to evaluate antigen-specific T cell responses also do not use negative control peptides^{22,23}. Cultures were split and IL-2 medium was replenished as needed on days 4, 7 and 10 of culture.

To determine the cytokine potential of activated T cells, autologous antigen-presenting cells (APCs) were prepared for T cell restimulation on day 10. Thawed PBMCs were labeled with anti-CD2-biotin antibodies (Biolegend) in cold MACS buffer (PBS, 0.5% BSA, 2 mM EDTA), and CD2-positive T cells and natural killer cells were depleted using Streptavidin MyOne T1 Dynabeads (Life Technologies). The CD2-negative fraction comprising predominantly blood monocytes was cultured in 96-well round-bottom plates at 1 × 10³–1.5 × 10⁵ cells/well in the presence of recombinant Cas proteins, GFP, ovalbumin (5 µg/ml) or peptides from RfxCas13d, SpCas9 or viral peptide pools, as above for antigen capture. After 16–18 hours, expanded T cells were added to the APCs for restimulation in the presence of anti-CD28 antibody (1 µg/ml, LEAF-purified, Biolegend). To assess cytokine production, brefeldin A (10 µg/ml, eBioscience, Life Technologies) and monensin (2 µM, eBioscience, Life Technologies) were added to cultures 4–6 hours before staining for flow cytometric analysis. For peptide expansion and stimulation experiments, anti-CD107a PE antibody (Biolegend) was added into culture for 1 hour at 37°C before brefeldin A and monensin were added. For positive controls, T cells expanded with viral peptides were re-stimulated by adding to APCs cultured in the presence of viral peptides. Some cells expanded using viral peptides were separately stimulated with phorbol 12-myristate 13-acetate (PMA) and ionomycin (Cell Stimulation Cocktail, eBioscience, Life Technologies) as flow-cytometry controls. To ensure that cytokine-producing cells were indeed expanded by 10 day cultures, PBMCs cultured for 10 days without antigen were also restimulated with APCs that had captured protein or peptide antigen in the presence of anti-CD28 antibody to determine baseline non-antigen-specific cytokine production. Any detected responses were subtracted as background. All donors showed increased proliferation and cytokine responses in T cells after Cas9 or Cas13 stimulation compared with GFP stimulation, demonstrating that we could detect Cas9- and Cas13-specific responses over and above any background residual host protein responses in all donors, thus supporting the inclusion of all donors for the T cell analysis.

Flow cytometry. Cultured cells were washed twice with FACS buffer (PBS, 2% FBS, 0.1% BSA, 2 mM EDTA, 0.01% sodium azide (S2002, Sigma-Aldrich)) and stained for flow cytometry, as has been described²⁰. Cells were incubated with Human Fc Block (BD) for 10–15 minutes on ice before staining antibodies were added. Antibodies used are listed in Supplementary Table 2. Cells were incubated with antibody mixes for 20–30 minutes on ice and washed twice before acquisition. For intracellular cytokine staining, cells were fixed and permeabilized with Cytofix/Cytoperm solution (BD) for 20 minutes on ice, then washed with Perm/Wash buffer (BD). Cells were stained with intracellular staining antibodies in Perm/Wash Buffer for 20 minutes on ice, then washed twice before acquisition. Cells were acquired on LSR Fortessa or X-20 (BD) using FACS DiVa software (Version 9, BD) and analyzed on FlowJo software (Version 10.8, BD).

Statistical analyses. ELISA data was analyzed using GainData (Arigo Biolaboratories, <https://www.arigobio.com/elisa-analysis>). Standards were plotted using 5 parameter logistic regression. Plasma was tested at 4 dilutions (1:20, 1:40, 1:80, 1:160) and readings were obtained within the linear region of the standard curve were used to calculate antigen-specific IgG concentrations. For all other data, GraphPad Prism 9 (Graphpad Software) was used for statistical analysis and

graphical representations. The appropriate statistical tests were chosen on the basis of experimental design after consulting the GraphPad Statistics Guide.

Homology analysis. Protein sequence for RfxCas13d (accession number: [SFX39573.1](#)) was aligned with one of the top hits found using NCBI Protein Blast, Cas13d from a human gut isolate *Ruminococcus sp.* AM28-13 (accession number: [WP_117925375.1](#)). Alignment was completed using Clustal W (1.83) on EBI tools and alignment figure was generated in Jalview²⁴.

Reporting summary. Further information on research design is available in the Nature Research Reporting summary linked to this article.

Data availability

Source data are available for Figs. 1 and 2 and Extended Data Figs. 1, 3, and 4–6. The raw SDS-PAGE gel images for the purified Cas enzymes and GFP are provided in Supplementary Fig. 1. Flow cytometry data has been deposited in Flow Repository. (<http://flowrepository.org/id/RvFrbljuBY5uDR7bGwyHHFMjY5JhNlSrtMZ5dqhdPHz8MyoB5j91O8bhvSaNMIRy> and <http://flowrepository.org/id/RvFrmivRKvtmNgusJBRON7bHfEHGIS4HJvikD0t5FWuuVU8Cscfj00je6LkWbD>) Source data are provided with this paper.

Code availability

No custom codes were used in this study.

References

20. Tang, X.-Z., Kreuk, L. S. M., Cho, C., Metzger, R. J. & Allen, C. D. C. Bronchus-associated macrophages are positioned for soluble antigen capture from the airway lumen and for local T_H2 cell activation. Prprint at *bioRxiv* <https://doi.org/10.1101/2020.09.18.247742> (2020).
21. Gehring, A. J. et al. Licensing virus-specific T cells to secrete the neutrophil attracting chemokine CXCL-8 during hepatitis B virus infection. *PLoS ONE* **6**, e23330 (2011).
22. Le Bert, N. et al. SARS-CoV-2-specific T cell immunity in cases of COVID-19 and SARS, and uninfected controls. *Nature* **584**, 457–462 (2020).
23. Swadling, L. et al. Pre-existing polymerase-specific T cells expand in abortive seronegative SARS-CoV-2. *Nature* **601**, 110–117 (2022).
24. Waterhouse, A. M., Procter, J. B., Martin, D. M., Clamp, M. & Barton, G. J. Jalview Version 2—a multiple sequence alignment editor and analysis workbench. *Bioinformatics* **25**, 1189–1191 (2009).

Acknowledgements

We thank A. Bertoletti and A. Tan for valuable feedback on the manuscript. We thank the staff at flow cytometry core facility (Life Science Institute, Immunology Programme, NUS) for their assistance. This project was supported by the Singapore National Research Foundation (NRF) Research Fellowship (NRFVI2017-01-01, G. W. Y) and the Agency for Science, Technology and Research (H17/01/a0/012, S. H.). The funders had no role in study design, data collection, and analysis, decision to publish, or preparation of the manuscript.

Author contributions

X.-Z.E.T. conceived the study, designed and conducted the experiments, analyzed the data and wrote the manuscript. S.X.T. conducted the experiments and analyzed the data. S.H. and G.W.Y. conceived the study, designed the experiments and wrote the manuscript.

Competing interests

G.W.Y. is co-founder, member of the Board of Directors, a scientific advisor, equity holder and paid consultant for Locanabio. G.W.Y. is a visiting professor at the National University of Singapore. All other authors declare no competing financial interests.

Additional information

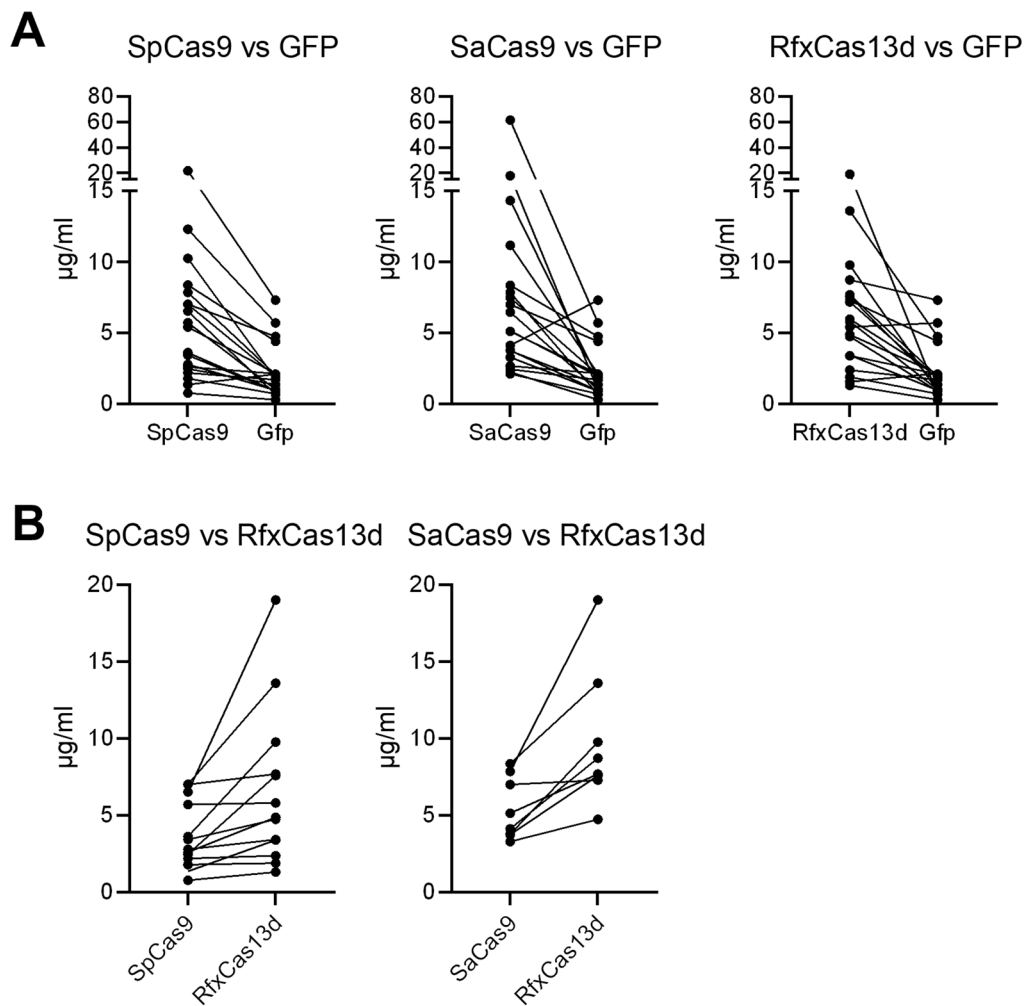
Extended data is available for this paper at <https://doi.org/10.1038/s41591-022-01848-6>.

Supplementary information The online version contains supplementary material available at <https://doi.org/10.1038/s41591-022-01848-6>.

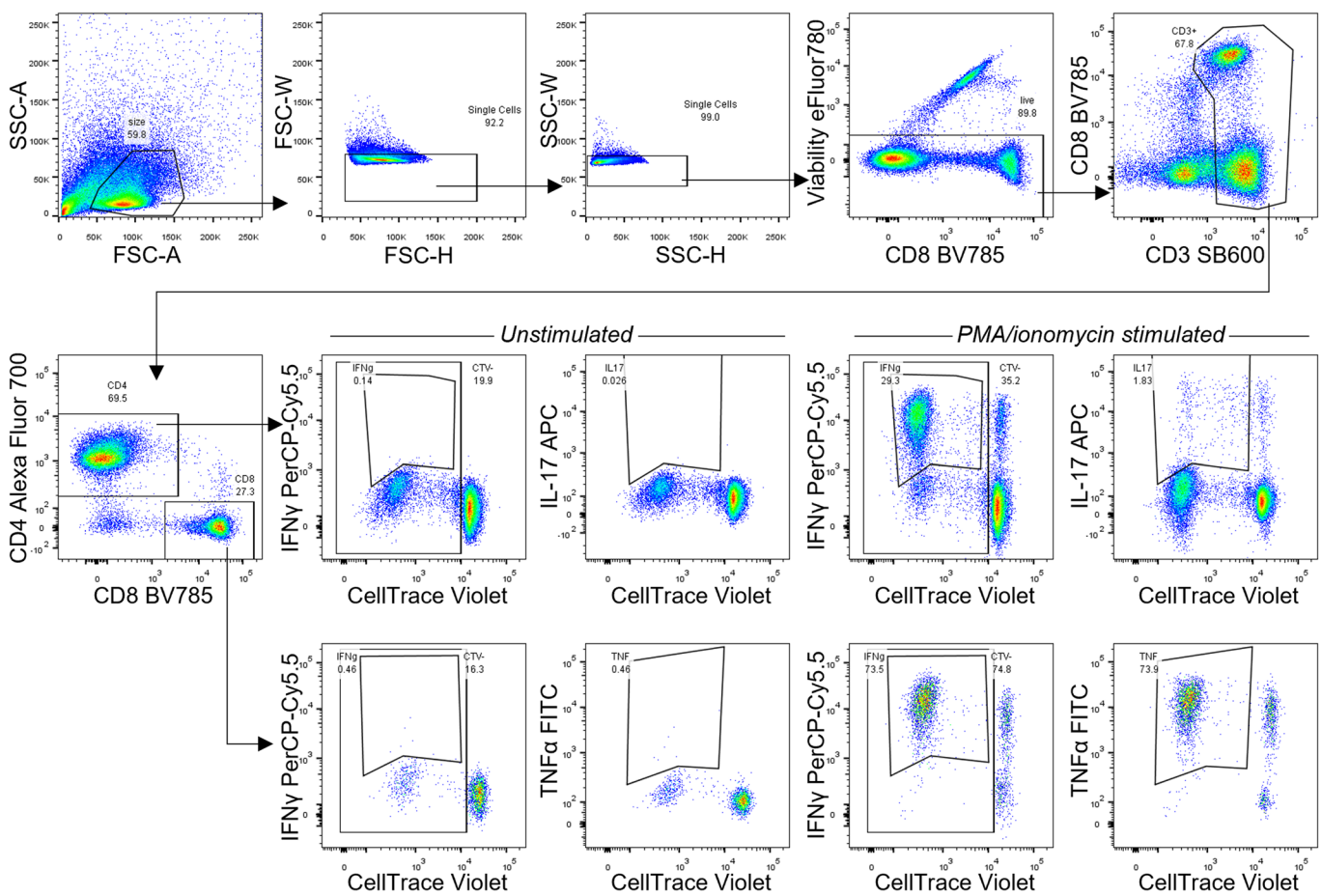
Correspondence and requests for materials should be addressed to Gene W. Yeo.

Peer review information *Nature Medicine* thanks Hui Yang and the other, anonymous, reviewer(s) for their contribution to the peer review of this work. Primary Handling editors: Saheli Sadanand and Anna Maria Ranzoni, in collaboration with the *Nature Medicine* team.

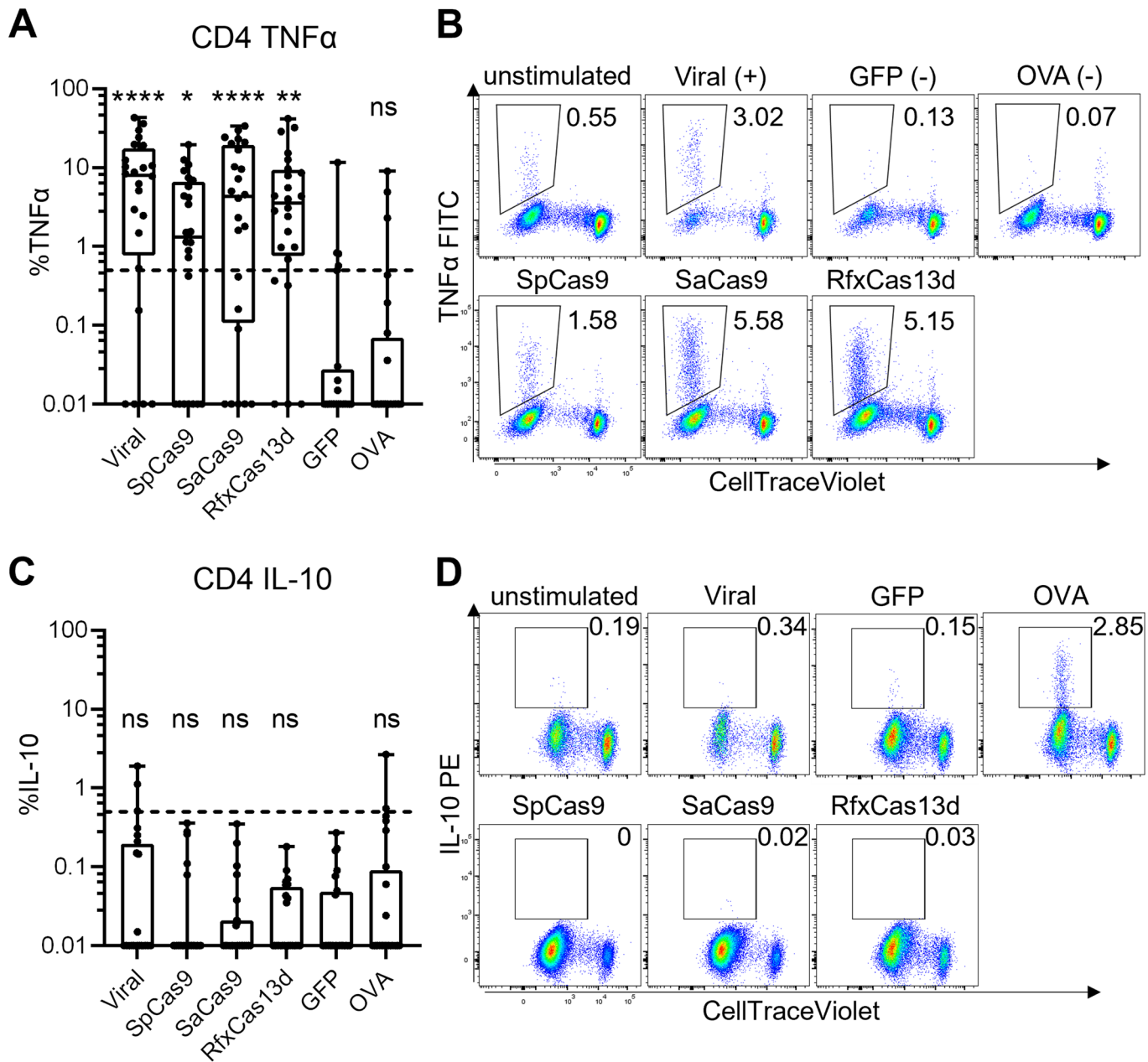
Reprints and permissions information is available at www.nature.com/reprints.



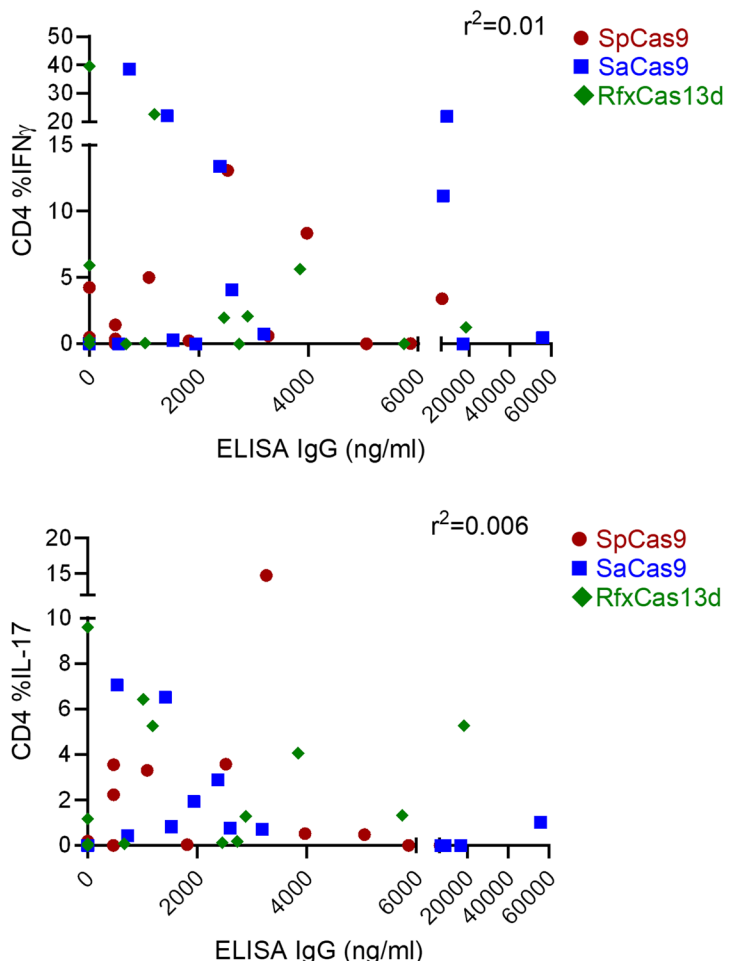
Extended Data Fig. 1 | Paired comparisons of IgG antibody response between recombinant proteins. (a) Paired data comparing IgG antibody responses detected against each of the Cas proteins with GFP control protein. All analyzed samples shown ($n=19$ biologically independent samples). (b) Paired data showing samples with higher IgG antibody responses against RfxCas13d compared to SpCas9 ($n=13$) or SaCas9 ($n=8$).



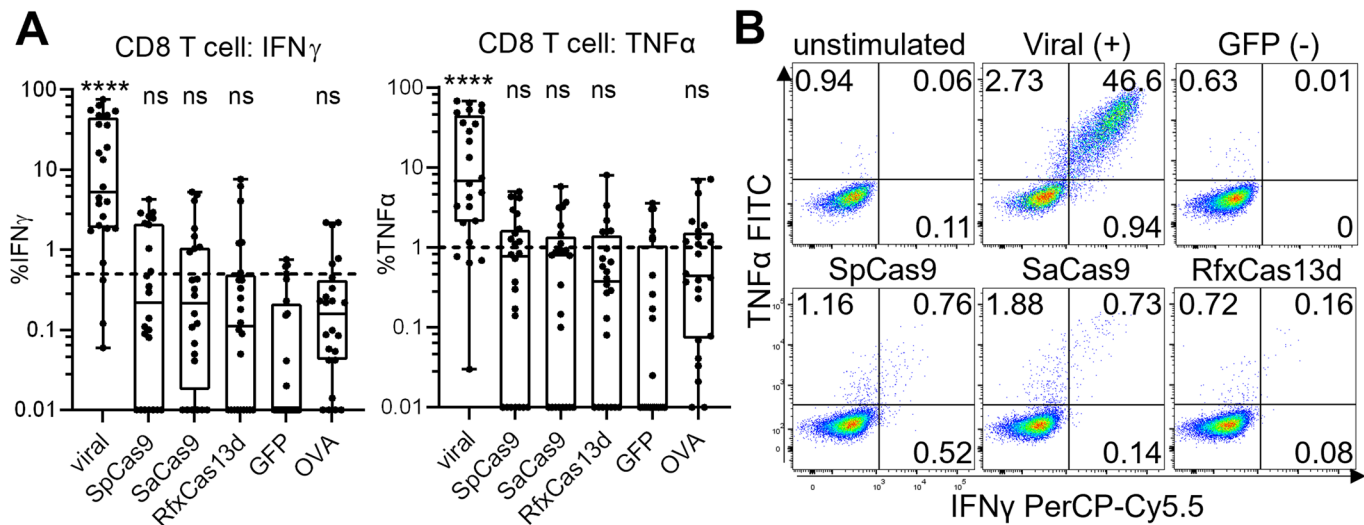
Extended Data Fig. 2 | Gating strategy for flow cytometry.



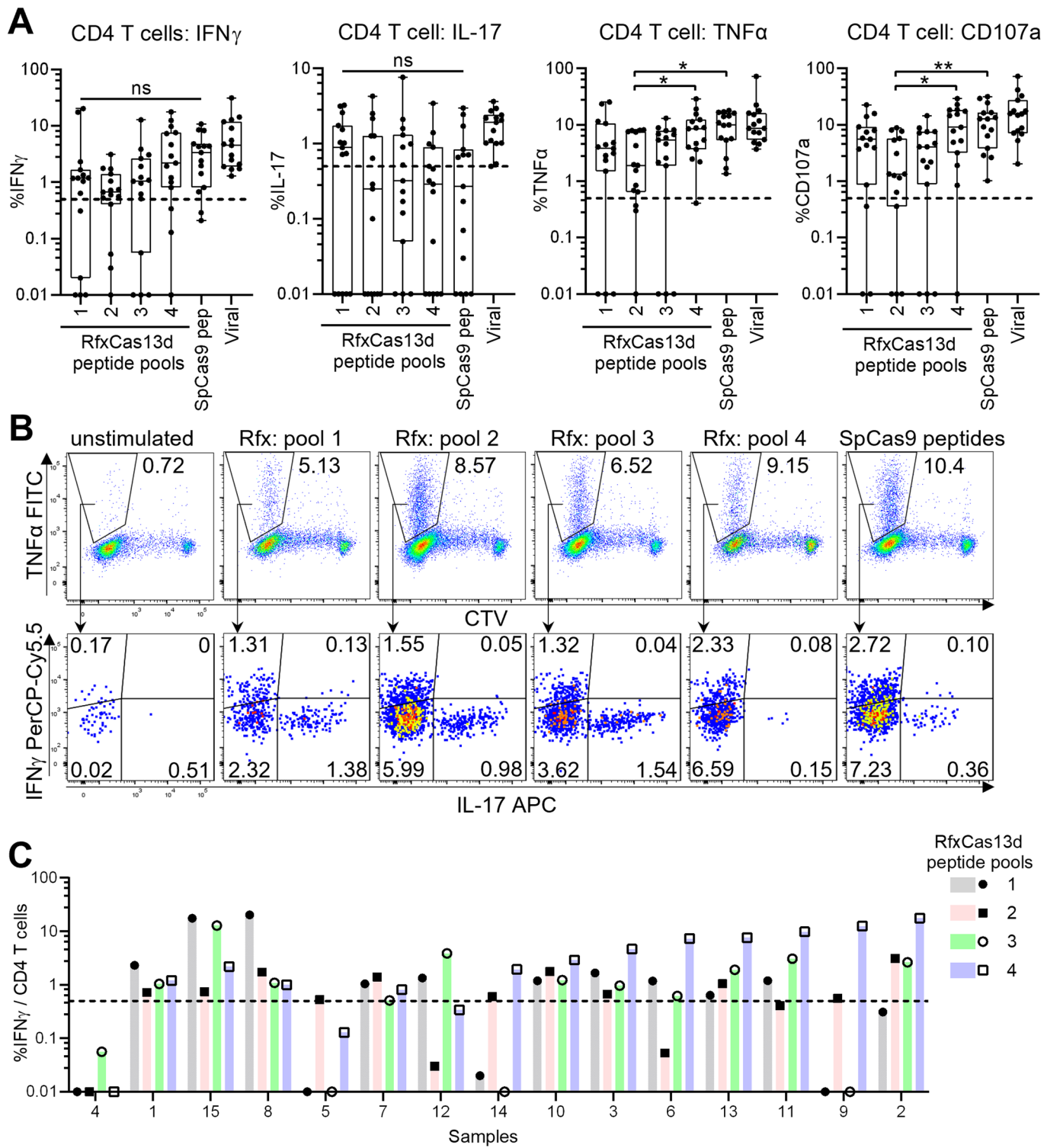
Extended Data Fig. 3 | TNF α and IL-10 in CD4 T cells stimulated with recombinant Cas proteins. TNF α (**a, b**) and IL-10 (**c, d**) responses in CD4 T cells expanded with recombinant Cas proteins over 10 days and restimulated on the last day of culture. (**a, c**) Aggregate responses are shown, with each data point representing one sample. ($n=23$ biologically independent samples). Each sample was tested across all conditions shown. To ensure cytokine responses are indeed from cells expanded by antigen stimulation, each data point plots values after subtracting background responses from controls expanded with no antigen but re-stimulated with the tested antigen. Differences in treatment conditions were tested using Friedman's test with two-sided Dunn's multiple comparisons test using GFP as the control. (ns, not significant, * $p < 0.05$, ** $p < 0.01$, *** $p < 0.001$, **** $p < 0.0001$). For box-plots, center line indicates median, box limits indicate 25th and 75th percentiles, whiskers show minimum to maximum value. Dashed line indicates the limit of detection for antigen specific responses. (**b, d**) Representative flow cytometric analysis of cytokine responses from one sample is shown.



Extended Data Fig. 4 | Correlation between antibody and CD4 T cell responses to recombinant Cas proteins. Frequency of CD4 T cell IFN γ (top) or IL-17 (bottom) responses were plotted against the corresponding IgG antibodies detected recognizing each of the Cas proteins in 13 samples in which paired data was available. T cell values reported are obtained after subtracting background responses from controls expanded with no antigen but re-stimulated with the tested antigen. IgG values reported are obtained after subtracting background responses from GFP controls.



Extended Data Fig. 5 | Cytokine profile of recombinant protein-stimulated RfxCas13d-specific CD8 T cells. (a) Aggregate responses are shown, with each data point representing one sample. ($n=23$ biologically independent samples). Each sample was tested across all conditions shown. To ensure cytokine responses are indeed from cells expanded by antigen stimulation, each data point plots values after subtracting background responses from controls expanded with no antigen but re-stimulated with the tested antigen. Differences in treatment conditions were tested using Friedman's test with two-sided Dunn's multiple comparisons test using GFP as the control. (ns, not significant, * $p < 0.05$, ** $p < 0.01$, *** $p < 0.001$, **** $p < 0.0001$). For box-plots, center line indicates median, box limits indicate 25th and 75th percentiles, whiskers show minimum to maximum value. Dashed line indicates the limit of detection for antigen specific responses. (b) Representative flow cytometric analysis of cytokine responses from one sample is shown.



Extended Data Fig. 6 | Cytokine profile of peptide-stimulated RfxCas13d specific CD4 T cells. (a) Aggregate responses are shown, with each data point representing one sample. ($n=15$ biologically independent samples). Each sample was tested across all conditions shown. To ensure cytokine responses are indeed from cells expanded by peptide stimulation, each data point plots values after subtracting background responses from controls expanded with no peptide (DMSO) but re-stimulated with the tested peptide pool. For box-plots, center line indicates median, box limits indicate 25th and 75th percentiles, whiskers show minimum to maximum value. Dashed line indicates the limit of detection for peptide specific responses. Differences in treatment conditions were tested using Friedman's test with two-sided Dunn's multiple comparisons test across the SpCas9 and 4 RfxCas13d peptide pools. (ns, not significant, * $p < 0.05$, ** $p < 0.01$). (b) Representative flow cytometric analysis of cytokine responses from one sample is shown, indicating the detection of IFN γ and IL-17 responding cells within the TNF α producing proliferated cell population. Percentages shown are frequency among total CD4 T cells. (c) CD4 T cell IFN γ responses from each sample is shown. Samples are sorted based on the peptide pool which elicited the strongest responses.

RfxCas13d/1-967	1	- - - - - MIEKKKSFAKGGMGVK	15
AM28-13/1-922	1	MAKKKNKMKPRELREAQKKARQLKAAEINNNNAVPAIAAMPAAEAAAPAEKKKSSVKAAGMK	61
RfxCas13d/1-967	16	STLVS GSKVYMTTFAEGSDARLEKIVEGDSIR- - SVNEGEAFSAEMADKNAGYKIGNAKFS	74
AM28-13/1-922	62	SILVSENKMYITSFGKGNSAVLEYEVNDNDYNKTQLSSKDNSNIELCDVDEVNITFSSKG	122
RfxCas13d/1-967	75	HPKG YAVVANNPLY - - - TGPVQQDMLGLKETLEKRYFGESADGNNDNICIQVIHNILDIEK	131
AM28-13/1-922	123	FESGVKINTSNPNTHRSGESSSVRGDMLGLKSELEKRF FGKTFD - - DNIHIQLIYNILDIEK	181
RfxCas13d/1-967	132	I LAEYITNAAYAVNNISGLD - - - KDIIGFGKFSTVYTYDEFKDPEHHRAAFNNNDKLINA	188
AM28-13/1-922	182	I LAVYVVTNIVYALNNMLGLENESNNDFMGY - - LSAKNTYDVFTDPDESDSLKN - - - IKGN	236
RfxCas13d/1-967	189	IKAQYDEFDNFLDNPRLGYFGQAFFSKEGRNYIINYGNECYDILALLSGLRHWWVHNNEEE	249
AM28-13/1-922	237	IKKSLSKFNDLLKTKRLGYFGLEEPKTDKRVEASYKKRVYHMLAIVGQIRQSVFHDKSNE	297
RfxCas13d/1-967	250	SRSIRTWLYNLDKNLDNEYISTLNLYDRITNTELNSFSKNSAANVNVI AETL - - GINPAE	308
AM28-13/1-922	298	- - LDEYLYSFIDIIDSEYRETLDYLIDERFDSINKGFIQGNKVNVISLLIDMMKDDYEADD	355
RfxCas13d/1-967	309	FAEQYFRFSIMKEQKNLGFNTKLRREVMLDRKDMSEIRKNHKVFDSIRTKVYTMMDFVIYR	369
AM28-13/1-922	356	IIRLYYDFIVLKSQKNLGFSIKKLREKMLDEYG - - FRFKDKQYDSVRSKMYKLMDFLFC	413
RfxCas13d/1-967	370	YYIEEDAKVAAANKSLPDNEKSLSEKDI FVINL RGSFNDDQKD ALYYDEANRIWRKLENIM	430
AM28-13/1-922	414	NYYRNNDVIAGEA - - - - - LVRKLRF SMTDDEKEGIYADEAAKLWGKFRNDF	458
RfxCas13d/1-967	431	HNIKE-FRGNKTR EYKKDAPRLPRILPAGR - - - DVSAFSKLMYALT MFLDGKEINDLLT	486
AM28-13/1-922	459	ENIADHMNGDV I KELGKADMDFDEKILDSEKKNASDLLYFSKMIYMLTYFLDGKEINDLLT	519
RfxCas13d/1-967	487	TLINKF DN IQSFLKVM - - PLIGVNAKFVEEYAFFKDSAKIADELRLIKSFARMGEPIADAR	545
AM28-13/1-922	520	TLISKFDNIKEFLKIMKSSAVNVECELTAGYKLFDNSQRITNELFIVKNIASMRKPAAASK	580
RfxCas13d/1-967	546	RAMYIDAIRILGTNLSYDEL - - KALADTFSLDENGNKLLKGKHGMRFNIIINNISNKRHY	604
AM28-13/1-922	581	LTMFRDALTI LGID - - DKITDDR ISEILKLKEKG - - - KGIGHGLRNFITNNVIESSRFVY	634
RfxCas13d/1-967	605	LIRYGDPAHLHEIAKNEAVVKFVLGRIADIQKKQGQNGKNQIDRYYETCIG-KDKGKSVSE	664
AM28-13/1-922	635	LIKYANAQKIREVAENEKVVMFVLGGIPD - - - - - TQIERYYKSCVEFPDMNSSLEV	685
RfxCas13d/1-967	665	KVDALT KIIITGMNYDQFDKKRSVIEDTGREN AEREKFKKIISLYLTVIYHILKNIVNINAR	725
AM28-13/1-922	686	KRSELARM IKNIRFDFFKVNQK - - QAKGRENAVAKERAKAVIGLYLTVMYLLVKNLVNVNAR	744
RfxCas13d/1-967	726	YYVIGFHCVERDAQLYKEKG YDINLKLEEKGFSSVTKL CAGIDETAPDKRDVEKEMAERA	786
AM28-13/1-922	745	YYVIAIHCLERDFGLYKEIIPELASKNLKNDYRILSQ TLC - - - - - ELCDNG	789
RfxCas13d/1-967	787	KESIDSLESANPKLYANYIKYSDEKKAEFTRQINREKAKTALNAYLRNTKWNVIIRE DLL	847
AM28-13/1-922	790	DES - - - - - PNLFLK - - - - - KNRRRLRKCVEVDIN	812
RfxCas13d/1-967	848	RIDNKTCTLFRNKAVHLEVARYVHAYINDIAEVNSYFQLYHYIMQRILIMNERYEKSSGKVS	908
AM28-13/1-922	813	NADSSMTRKYRNCIAHLT VVRELKEYIGDIRTVDSYFSIYHYVMQRCITKREDDTKQEDKI	873
RfxCas13d/1-967	909	EYFDAVNDEKKYNDRLLKLCVPFGYCIPRFKNLSIEALFDRNEAAKFDKEKKKVSGNS	967
AM28-13/1-922	874	KYEDDLKNHGYTKDFVKALNSPFGYNIPRFKNLSIEQLFDRNE - - - YLTEK - - - -	922

Extended Data Fig. 7 | Homology between RfxCas13d and human gut isolate *Ruminococcus* sp. AM28-13. Protein sequence alignment between RfxCas13d (top row) and human gut isolate AM28-13 (bottom row) with dark blue boxes highlighting homologous amino acids.

Corresponding author(s): Gene Yeo

Last updated by author(s): Apr 12, 2022

Reporting Summary

Nature Portfolio wishes to improve the reproducibility of the work that we publish. This form provides structure for consistency and transparency in reporting. For further information on Nature Portfolio policies, see our [Editorial Policies](#) and the [Editorial Policy Checklist](#).

Statistics

For all statistical analyses, confirm that the following items are present in the figure legend, table legend, main text, or Methods section.

n/a Confirmed

- The exact sample size (n) for each experimental group/condition, given as a discrete number and unit of measurement
- A statement on whether measurements were taken from distinct samples or whether the same sample was measured repeatedly
- The statistical test(s) used AND whether they are one- or two-sided
Only common tests should be described solely by name; describe more complex techniques in the Methods section.
- A description of all covariates tested
- A description of any assumptions or corrections, such as tests of normality and adjustment for multiple comparisons
- A full description of the statistical parameters including central tendency (e.g. means) or other basic estimates (e.g. regression coefficient) AND variation (e.g. standard deviation) or associated estimates of uncertainty (e.g. confidence intervals)
- For null hypothesis testing, the test statistic (e.g. F , t , r) with confidence intervals, effect sizes, degrees of freedom and P value noted
Give P values as exact values whenever suitable.
- For Bayesian analysis, information on the choice of priors and Markov chain Monte Carlo settings
- For hierarchical and complex designs, identification of the appropriate level for tests and full reporting of outcomes
- Estimates of effect sizes (e.g. Cohen's d , Pearson's r), indicating how they were calculated

Our web collection on [statistics for biologists](#) contains articles on many of the points above.

Software and code

Policy information about [availability of computer code](#)

Data collection Flow cytometric data was collected using FACS DiVa (BD) software. No custom code was used.

Data analysis ELISA data was analyzed using GainData (Arigo Biolaboratories). Flow cytometric data was analysed using FlowJo (V10.8, BD). Statistical analysis and graphical representations were done using Prism (V9, GraphPad). Protein sequence for RfxCas13d (Accession Number: SFX39573.1) was aligned with one of the top hits found using NCBI Protein Blast, Cas13d from a human gut isolate Ruminococcus sp. AM28-13 (Accession Number: WP_117925375.1). Alignment was completed using Clustal W (1.83) on EBI tools and alignment figure was generated in Jalview. No custom code was used.

For manuscripts utilizing custom algorithms or software that are central to the research but not yet described in published literature, software must be made available to editors and reviewers. We strongly encourage code deposition in a community repository (e.g. GitHub). See the Nature Portfolio [guidelines for submitting code & software](#) for further information.

Data

Policy information about [availability of data](#)

All manuscripts must include a [data availability statement](#). This statement should provide the following information, where applicable:

- Accession codes, unique identifiers, or web links for publicly available datasets
- A description of any restrictions on data availability
- For clinical datasets or third party data, please ensure that the statement adheres to our [policy](#)

Source data are available for Figures 1 and 2 and Extended Data Figures 1, 3, 4, 5, 6. The raw SDS-PAGE gel images for the purified Cas enzymes and GFP are provided in Supplementary Figure 1. Flow cytometry data has been deposited in Flow Repository. (<http://flowrepository.org/id/>)

Field-specific reporting

Please select the one below that is the best fit for your research. If you are not sure, read the appropriate sections before making your selection.

Life sciences Behavioural & social sciences Ecological, evolutionary & environmental sciences

For a reference copy of the document with all sections, see nature.com/documents/nr-reporting-summary-flat.pdf

Life sciences study design

All studies must disclose on these points even when the disclosure is negative.

Sample size	We used a sample size of 15-24 samples. No sample size calculation was performed. This study intends to obtain a general idea of whether the healthy human population possess pre-existing immunity recognizing the antigens tested and does not intend to define exact prevalence or confidence intervals. We analysed samples as they were collected for the ELISA and protein stimulation assays, and stopped when additional samples did not alter trends observed. From the protein stimulation assays, we found that 15 samples were sufficient to establish trends, therefore 15 samples were analysed for the peptide stimulation assays.
Data exclusions	For ELISA, data were excluded if responses to GFP were unusually high, indicating that there may be other substances within the protein preparation or plasma sample that may be non-specifically inducing HRP activity. In such situations, any responses observed could not be reliably attributed to the specific protein antigen. For flow cytometry, no data were excluded.
Replication	The assay was repeated in 3 individual samples and all 3 samples showed similar results upon replication, ensuring that the results are reproducible.
Randomization	There are no experimental groups, all samples were assayed the same way.
Blinding	Investigators are blind to all donor demographic information. All samples are assayed the same way with no separation into experimental groups.

Reporting for specific materials, systems and methods

We require information from authors about some types of materials, experimental systems and methods used in many studies. Here, indicate whether each material, system or method listed is relevant to your study. If you are not sure if a list item applies to your research, read the appropriate section before selecting a response.

Materials & experimental systems		Methods	
n/a	Involved in the study	n/a	Involved in the study
<input type="checkbox"/>	<input checked="" type="checkbox"/> Antibodies	<input checked="" type="checkbox"/>	<input type="checkbox"/> ChIP-seq
<input checked="" type="checkbox"/>	<input type="checkbox"/> Eukaryotic cell lines	<input type="checkbox"/>	<input checked="" type="checkbox"/> Flow cytometry
<input checked="" type="checkbox"/>	<input type="checkbox"/> Palaeontology and archaeology	<input checked="" type="checkbox"/>	<input type="checkbox"/> MRI-based neuroimaging
<input checked="" type="checkbox"/>	<input type="checkbox"/> Animals and other organisms		
<input type="checkbox"/>	<input checked="" type="checkbox"/> Human research participants		
<input checked="" type="checkbox"/>	<input type="checkbox"/> Clinical data		
<input checked="" type="checkbox"/>	<input type="checkbox"/> Dual use research of concern		

Antibodies

Antibodies used	Details for antibodies used are available in Supplementary Table 2 as part of the manuscript files.
Validation	Antibodies were validated by manufacturers and available for each clone on their website, links for each antibody is provided in Supplementary Table 2.

Human research participants

Policy information about [studies involving human research participants](#)

Population characteristics	No information regarding the demographic of the human blood donors are known to the investigators.
Recruitment	The donors were recruited independently by the Singapore Health Sciences Authority as platelet blood donors who are otherwise healthy. Investigators receive residual blood cones that are otherwise discarded and are blinded to any profile of the blood donors. Singapore Health Sciences Authority obtains informed consent for the use of residual cone blood in

research. There is no compensation for participants. There may be self selection bias among donors but this would otherwise not impact the results.

Ethics oversight

Institutional Review Board at National University of Singapore (NUS) and at Agency for Science, Technology and Research (A*STAR), Singapore.

Note that full information on the approval of the study protocol must also be provided in the manuscript.

Flow Cytometry

Plots

Confirm that:

- The axis labels state the marker and fluorochrome used (e.g. CD4-FITC).
- The axis scales are clearly visible. Include numbers along axes only for bottom left plot of group (a 'group' is an analysis of identical markers).
- All plots are contour plots with outliers or pseudocolor plots.
- A numerical value for number of cells or percentage (with statistics) is provided.

Methodology

Sample preparation

Samples were obtained by plasmapheresis and PBMCs were isolated from residual cone blood by Ficoll density centrifugation. Details are available in the methods section.

Instrument

The data was acquired on LSR Fortessa or X-20 from Becton Dickinson. (BD).

Software

The data was collected using FACS DiVa software (BD) and analyzed on FlowJo Software (Treestar, BD).

Cell population abundance

We did not sort cells.

Gating strategy

Please see Extended Data Figure 2. In brief, FSC and SSC gates were set for lymphocytes, followed by H vs W gates for singlets in both FSC and SSC. Next we gated for Live cells, followed by CD3+ T cells and distinct gates for CD4 and CD8 T cells. Subsequently CTV, IFNg, IL-17 and TNFa gates were set within the CD4 and CD8 T cell populations, using unstimulated cells (negative) and PMA/ionomycin stimulated cells (positive) to define the boundaries between negative and positive cells.

Tick this box to confirm that a figure exemplifying the gating strategy is provided in the Supplementary Information.